

Phase Synchronization in Railway Timetables

Christoph Fretter¹, Lachezar Krumov², Karsten Weihe², Matthias Müller-Hannemann¹, and Marc-Thorsten Hütt³ ^a

¹ Institut für Informatik, Martin-Luther-Universität Halle-Wittenberg, Halle, Germany

² Fachgebiet Algorithmik, Technische Universität Darmstadt, Darmstadt, Germany

³ School of Engineering and Science, Jacobs University, Bremen, Germany

Received: date / Revised version: date

Abstract. Timetable construction belongs to the most important optimization problems in public transport. Finding optimal or near-optimal timetables under the subsidiary conditions of minimizing travel times and other criteria is a targeted contribution to the functioning of public transport. In addition to efficiency (given, e.g., by minimal average travel times), a significant feature of a timetable is its robustness against delay propagation. Here we study the balance of efficiency and robustness in long-distance railway timetables (in particular the current long-distance railway timetable in Germany) from the perspective of synchronization, exploiting the fact that a major part of the trains run nearly periodically. We find that synchronization is highest at intermediate-sized stations. We argue that this synchronization perspective opens a new avenue towards an understanding of railway timetables by representing them as spatio-temporal phase patterns. Robustness and efficiency can then be viewed as properties of this phase pattern.

PACS. 89.75.Fb Structures and organization in complex systems – 89.75.Hc Networks and genealogical trees – 89.20.Ff Computer science and technology – 89.40.-a Transportation

1 Introduction

Railway timetables should be designed to achieve a maximum level of utilization from a passenger’s perspective. That is, regular waiting times for connecting trains should be kept to a minimum. However, this limits the network’s robustness against perturbations: Depending on the waiting policy among connecting trains, a single delayed train may cause a cascade of further train delays in remote parts of the network. Minimal regular waiting times (minimal buffering times) cause maximal risk of such delay propagation. Understanding this trade-off and limiting the propagation of delays through the networks is a challenge of practical importance.

The construction of periodic railway timetables is algorithmically difficult and has been intensively studied as a periodic event scheduling problem (PESP), see for example [34, 29, 20]. The technical and economical side constraints for a valid non-periodic schedule can be modeled as a feasible differential problem on a directed graph $G = (V, E)$ with lower and upper edge bounds $\ell, u \in \mathbb{Q}^E$. In a basic model, the vertex set V corresponds to departure and arrival events, while the directed edges together with the bound values model constraints (travel times, minimum headway, minimum transfer times, etc.). One

seeks for a vector $\pi \in \mathbb{Q}^V$, called the timetable, which assigns to each event j a time-stamp π_j satisfying

$$\ell_e \leq \pi_j - \pi_i \leq u_e \text{ for all } e = (i, j) \in E.$$

Thus, lower and upper edge bounds restrict the difference between two timestamps from below and above, respectively. For example, $\ell_{(i,j)} = 15 \leq \pi_j - \pi_i$ means that event j has to occur at least 15 time units after event i . See Figure 1 for a small example.

In a periodic timetable, trains are grouped into lines which are to be operated by some period T . In the periodic event scheduling problem (with one fixed period T) one searches for a vector $\pi \in [0, T)$ such that for all $e = (i, j) \in E$ there exists $k_e \in \mathbb{Z}$ with

$$\ell_e \leq \pi_j - \pi_i + T \cdot k_e \leq u_e.$$

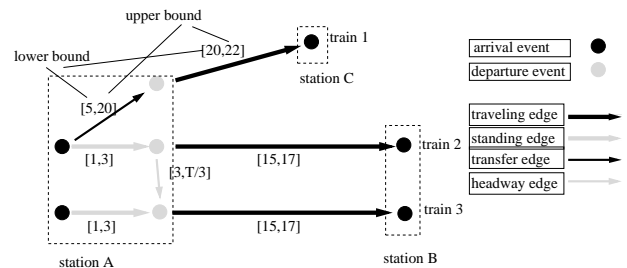


Fig. 1. Small excerpt of a periodic event scheduling problem.

^a supported by Volkswagen Foundation grants I/82717, I/82718 and I/83435. The authors wish to thank Deutsche Bahn AG for providing test data for scientific use.

For the local public transport in Berlin (Germany), the first optimized periodic timetable used in daily operation has been obtained using mixed-integer linear programming techniques [21]. Netherlands Railways also have recently introduced a completely new periodic timetable, generated by a number of sophisticated operations research techniques, including constraint programming [15]. For countries with a less periodic timetable, including Germany, the construction process for long-distance timetables is quite complex, and therefore still done to a large extent manually by experienced engineers. The planning process has a hierarchical component (international trains are scheduled first), and a behavioral component (keep as much as possible from the previous year’s schedule).

So far, railway timetables have been studied predominantly as an algorithmic challenge with the objective of constructing optimal (or near-optimal) connection patterns, minimizing resources and overall waiting time. Only recently, there have been first computational studies aiming at delay resistant periodic timetables [14, 22, 23].

Here we adopt an opposite perspective to timetable construction and analyze the spatio-temporal patterns induced by the timetable. A suitable language for this study is a representation of the train arrival/departure events as a spatio-temporal phase pattern. We study the distribution of synchronization across stations. Synchronization phenomena have received a lot of attention in traffic modeling over the last few years, in particular for car traffic in cities and the impact of traffic light synchronization on the formation of traffic jams [8, 18, 19].

In the case of railway timetables, the situation is different in several ways: The “load” of a station is essentially determined by the number of tracks (giving the maximal number of simultaneous or nearly simultaneous arrival/departure events). The typical number of directions (which can be interpreted as the degree of a station in a suitable effective network representation), from which one can select, is higher for train stations than for typical street crossings.

If one considers a network of long-distance train connections as a mesh of routes through a planar system, where trains are started periodically at the endpoints of these routes, the spatial distances between the intersection sites of these routes determine a spatio-temporal phase pattern. The free parameters of this pattern are the relative phases of the periodically started trains. In reality, the travel time between two stations can serve as an additional degree of freedom allowing for a shaping of the phase pattern beyond this simple thought experiment.

Our main hypothesis is that the rank of the stations sorted according to size is the organizing parameter (i.e. the “control parameter” from the perspective of self-organized systems [26, 31, 38]), along which synchronization can be understood. In this paper, we use the notion buffering time to denote the amount of time available to change between two trains (transfer time) for the planned schedule, i.e. without induced delays. Our other two observables are the average buffering time b_i at station i and the sec-

ondary delays $s_i(p)$ induced by a primary (incoming) delay p because trains have to wait for other trains.

The main result of our analysis is that a railway timetable induces a spatio-temporal phase pattern, and that properties of the phase pattern are linked to the efficiency and the robustness of the system. We observe that synchronization is highest at intermediate-sized stations.

Here we contribute two points to the general debate:

(1) We show that the current planning of railway timetables (which involves some algorithmic construction, some manual curation and the resorting to features from previous timetables) leads to an unexpected coherence on the level of the spatio-temporal phase pattern.

(2) At the same time, our analysis shows that the general concept of a spatio-temporal phase pattern is a novel and helpful view for network-based scheduling problems.

The remainder of this paper is structured as follows. In Section 2, we first give a detailed description of our numerical experiment, and then discuss the results in Section 3. Afterwards, we introduce an avalanche model for delay propagation on graphs (Section 4) helping us to understand the observed relation between synchronization and robustness. Finally, we conclude with a short summary and an outlook for future work (Section 5).

2 Formalism and Numerical Experiments

The quality of the timetable is related to two distinct (and often conflicting) objectives: The sum of travel times over all routes should be minimal (efficiency) and typical delays should minimally increase the overall travel time (robustness). Apart from some freedom to determine the planned travel time from one station to another (i.e. the prescribed average speed of the train), the main tuning capacity lies in the interchange time between connecting trains. While efficiency requires a minimization of interchange time, robustness can be established by using the interchange time as a buffer for incoming delays.

The secondary delays s_i observed at each station i across a range of primary delays p have been obtained by a large-scale numerical experiment performed on the actual timetable of Deutsche Bahn AG, together with real passenger information. Throughout our investigation we consider only long-distance train connections (served by the train categories ICE and IC/EC). To simulate the effects of delays, we use the dependency graph model introduced in [28] and its implementation within the fully realistic multi-criteria timetable information system MOTIS [33]. The dependency graph is basically a time-expanded graph model with distinct nodes for each departure and arrival event in the entire schedule for the current and following days. In addition, the model includes two further types of nodes: forecast and schedule nodes.

Each node has a time-stamp which can dynamically change. The timestamps reflect the current situation, i.e. the expected departure or arrival time subject to all delay information known up to this point. Schedule nodes are marked with the planned time of an arrival or departure event, whereas the time-stamp of a forecast node is

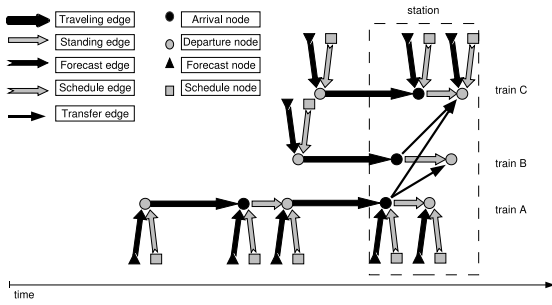


Fig. 2. Illustration of the dependency graph model (taken from [28]).

the current external prediction for its departure or arrival time.

The nodes are connected by five different types of edges (see Figure 2). The purpose of an edge is to model a constraint on the time-stamp of its head node.

- *Schedule edges* connect schedule nodes to departure or arrival nodes. They carry the planned time for the corresponding event of the head node (according to the published schedule).
- *Forecast edges* connect forecast nodes to departure or arrival nodes. They represent the time stored in the associated forecast node.
- *Standing edges* connect arrival events at a certain station to the following departure event of the same train. They model the condition that the arrival time of train t at station k plus its minimum standing time must be respected before the train can depart (to allow for boarding and disembarking of passengers).
- *Traveling edges* connect a departure node of some train t at a certain station k to the very next arrival node of this train at station k' .
- *Transfer edges* connect arrival nodes to departure nodes of other trains at the same station, if there is a planned transfer between these trains.

The current time-stamp for each departure or arrival node can be defined recursively, for details see [28].

The MOTIS tool can be used as follows. Given the planned train connection of a passenger and a concrete delay scenario (for example, a single primary delay of a train), we can query MOTIS for the fastest train connection towards the passenger’s destination, subject to the standard waiting rules between connecting trains. In particular, the train waiting regulations of Deutsche Bahn have been used. From the difference between the planned arrival time at the destination and the calculated arrival time in the delay scenario we obtain the individual delay for each passenger.

Passenger information has been available to us for a single day in the form of all travel agency bookings for that day. While these data are certainly distorted by the fact that most tickets are sold via vendor machines at the station (and these data have not been available to us), it

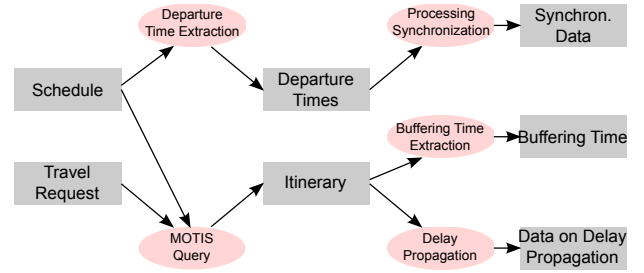


Fig. 3. Data flow in the delay propagation experiment.

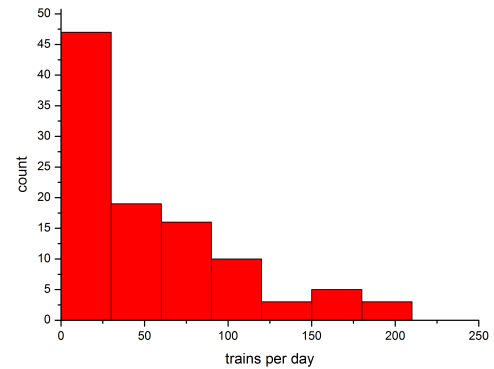


Fig. 4. Distribution of daily numbers of arrival/departure (A/D) events.

is nevertheless helpful to include passenger data for two reasons:

(1) Only routes, which have really been traveled, enter our analysis; in this way we avoid artifacts, e.g., from back-and-forth contributions.

(2) We can discuss both the average delay per passenger and the cumulative delay over all affected passengers (as a measure of the total systemic effect).

In Figure 3, we sketch the data flow within our numerical experiment, where we have processed 43772 train segments, 2622 stations, 130071 passenger routes, and about 1.8 million MOTIS queries.

In order to illustrate the raw data obtained from this numerical experiment, we show the station size distribution (where the station size is given by the number of arrival/departure events per day) in Figure 4; and the buffering time distribution in Figure 5. Both distributions are essentially unimodal and have a non-negligible tail at large values. The rare occurrence of low buffering times can be explained by the fact that the timetable information system does not provide connections where a (station-specific) minimal interchange time is not reached. It should be noted that this general rule is accompanied by a long list of exceptions for specific trains and specific connections. All these constraints and subsidiary conditions have been included in the numerical experiment, in order to obtain realistic event data.

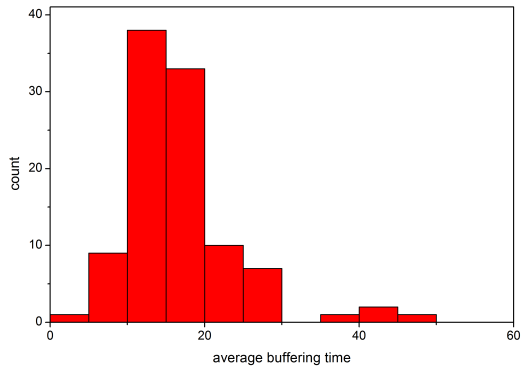


Fig. 5. Distribution of the average buffering time per station.

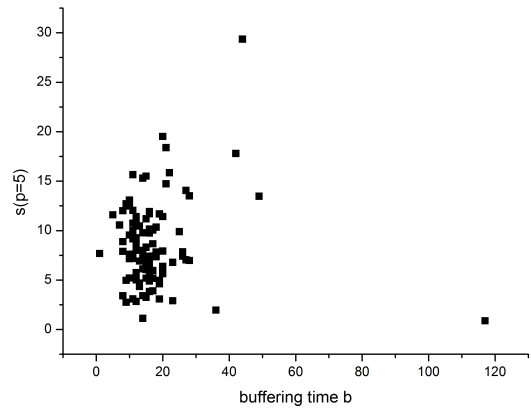


Fig. 7. Secondary delay as a function of the buffering time for a fixed primary delay $p = 5$ minutes, raw data.

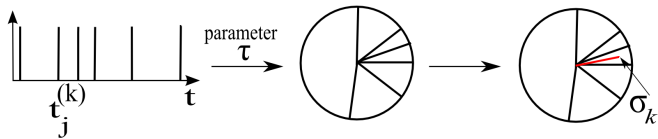


Fig. 6. Conversion of the arrival/departure times at a station k into the synchronization index σ_k .

As a next step we compare these delays with unperturbed features of the timetable. Our approach for converting the timetable into an event pattern uses the language of phase synchronization. Let $\{t_j^{(k)}, j = 1 \dots T_k\}$ be the set of arrival/departure (A/D) times $t_j^{(k)}$ of the j th train at station k . The quantity T_k denotes the number of A/D events at station k per day. These A/D times are now translated into phases

$$\phi_j^{(k)}(\tau) = \frac{2\pi}{\tau} (t_j^{(k)} \bmod \tau) \quad (1)$$

with the period length τ as a parameter. In our analysis we set this parameter to the maximal period length observed in the system, i.e., $\tau = 120$ minutes. For each station k we can now compute the synchronization index (as known from the classical studies of synchronization in populations of phase oscillators, see [16,36,39]; see also the scheme depicted in Figure 6):

$$\sigma_k = \sigma_k(\tau) = \left| \frac{1}{T_k} \sum_{j=1}^{T_k} e^{i\phi_j^{(k)}(\tau)} \right| \quad (2)$$

The view we want to propagate here, is that the performance (in a very general sense) of a given timetable of train connections is related to its phase pattern.

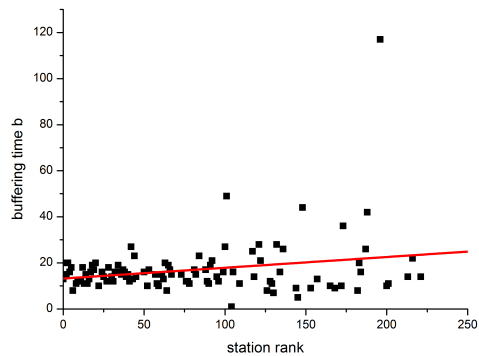


Fig. 8. Dependence of buffering time b on station rank.

3 Results

The large-scale numerical experiment described in the previous section in particular yields realistic values of the secondary (induced) delay $s(p)$ as a function of the primary (input) delay p . While at low p the value of $s(p)$ is mainly (but indirectly!) shaped by the buffering time b , at higher p the value is strongly influenced by the number of alternative connections.

On face value, one would expect a negative correlation of the secondary delay $s(p)$ and the buffering time b in this low- p region. In the raw data, Figure 7, there is rather a lack of correlation (or even a slight tendency towards positive correlations), which can be explained as follows: The buffering time b grows slowly with the station rank, i.e. decreases slightly with the station size (cf. Figure 8). At the same time, larger stations (i.e. more A/D events) offer more alternative routes, effectively reducing the secondary delay, even at low primary delay p .

In the example shown in Figure 9, there are only 4 minutes of buffering time which induce no delay. When p is in the range of [4, 9] minutes, the secondary delay becomes

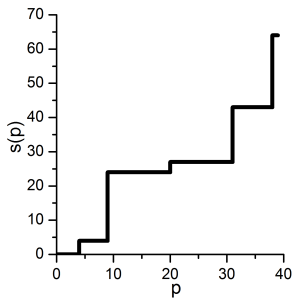


Fig. 9. Secondary delay as a function of the primary delay for a single train.

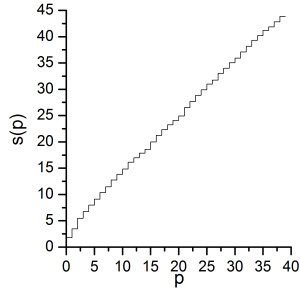


Fig. 10. Average secondary delay as a function of the primary delay for a single station (here: Frankfurt (Main) central).

4 minutes, and then jumps to 25 minutes. Figure 10 shows the average secondary delay at a station, which is, as a first approximation a linear function. At higher values of p , additional effects can be expected to set in:

- (1) with higher p more alternative routes become accessible,
- (2) more passengers will be affected, and
- (3) longer avalanches of delayed trains are triggered upon waiting.

These contributions are partially compensated by the waiting policy: Avalanche length is strongly reduced by maximal waiting times. Also, the second contribution has a smaller (but still non-zero) effect on the average secondary delay per passenger.

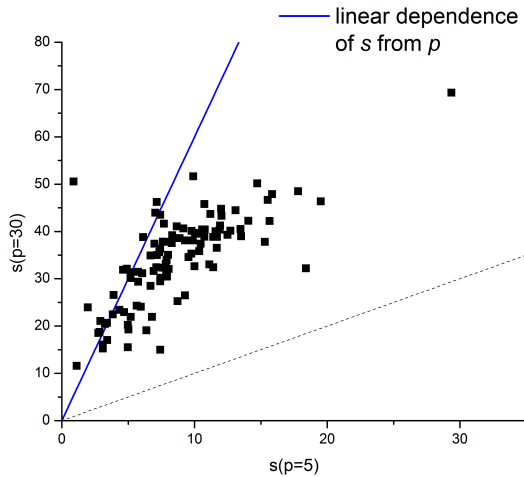


Fig. 11. Correlation of the secondary delay with primary delay of 5 and 30 minutes.

Figure 11 shows the correlation between the secondary delays for two different values of the primary delay, namely

$p=5$ minutes and $p=30$ minutes. There is a wide spread of deviations from the solid line showing the expectation for the case of a linear $s(p)$. This is indicative of the multitude of strengths with which these additional, higher- p effects contribute.

The challenge is now to establish in detail the relations between the degree of synchronization and the performance of the system (given by low delay propagation, i.e. robustness, and low overall transfer times, i.e. efficiency).

On the level of our data, the main performance indicators of the system, namely the efficiency and robustness, are only indirectly accessible via the secondary delays and the buffering times. We expect that a small $s(p)$ is related to high robustness (a given perturbation p induces a small effect s), while a small b can be associated with high efficiency (during a full itinerary only a small amount of time, given by the local buffering times b , is accumulated upon train interchanges).

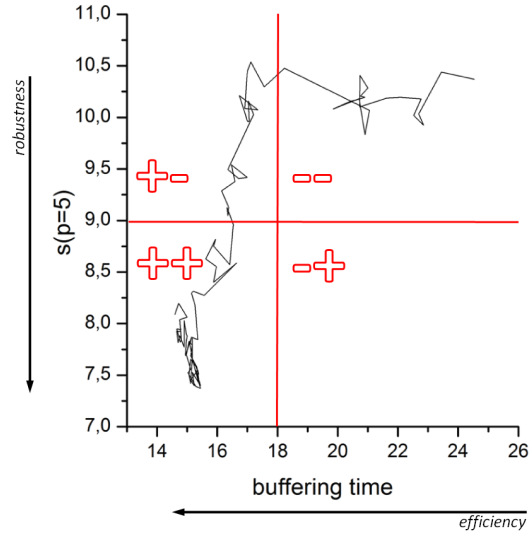


Fig. 12. Secondary delay as a function of the buffering time for a fixed primary delay $p = 5$ minutes, averaged and connected along the station rank, together with a phenomenological separation into quadrants according to high/low efficiency (first quadrant label) and high/low robustness (second label).

When splitting the b - $s(p)$ -plane into four quadrants corresponding of contributions of high/low delays and buffering times – and, consequently, low/high (–/+ performance –, one can observe very different usages (i.e., frequencies of occurrence in the data) of the quadrants:

The ++ region, which is the most efficient one as those stations are both efficient (small buffering time) and robust (small secondary delays), is most densely populated, followed by the +– region (high efficiency, low robustness). Very few stations are found in the –– region. Interestingly we do not find stations in the –+ region. Probably those are quickly eliminated during the schedule building or avoided during the route search.

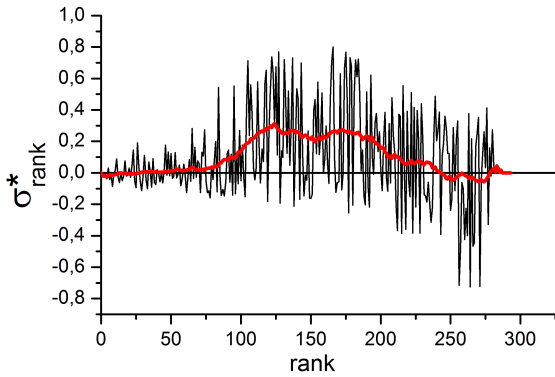


Fig. 13. The synchronization indices of the stations in ascending order of the station rank in Germany with $N_R = 100$ and an averaging window of 40

In order to better understand the systematic relation between $s(p)$ and b it is again helpful to use the station size as a control parameter along which local averages can be performed. The resulting curve is shown in Figure 12. This curve displays the backbone systematics of the interplay between efficiency (inverse b) and robustness (inverse $s(p)$) studied from the raw data in Figure 7, when using station size as an ordering parameter.

Figure 13 shows the synchronization index σ_k^* as a function of the station rank k . The phase data are distorted by the mere number of A/D events. In particular, at few A/D events large fluctuations of σ are induced. We therefore subtracted from each σ_k an average $\sigma_k^{(R)}$ over N_R runs of a null model, where the same number of A/D events has randomly been distributed in time. This procedure yields the reduced synchronization indices $\sigma_k^* = \sigma_k - \sigma_k^{(R)}$, shown as the black curve in Figure 13.

Furthermore, stations with neighboring ranks will differ (even though they are similar in size) in a variety of additional parameters. The original reduced synchronization index shows a strong local fluctuation along the rank. In order to eliminate the variation coming from these additional differences between similar-sized stations, we compute local averages over the σ_k^* . These values are shown as the red curve in Figure 13. Remarkably, synchronization is highest at intermediate station rank, decreasing towards both larger and smaller station sizes. In order to obtain this result, several processing steps of the raw data have been necessary. The systematic difference between the synchronization of large, small and intermediate train stations, respectively, is also seen, when average synchronization indices for each of these three categories are computed directly (Figure 14).

In order to assess, whether this elevated synchronization of intermediate-size stations is a property of train timetables beyond this individual case, we also computed the synchronization indices σ_k^* for four other counties, Austria, France, Norway, and the Czech Republic (Fig-

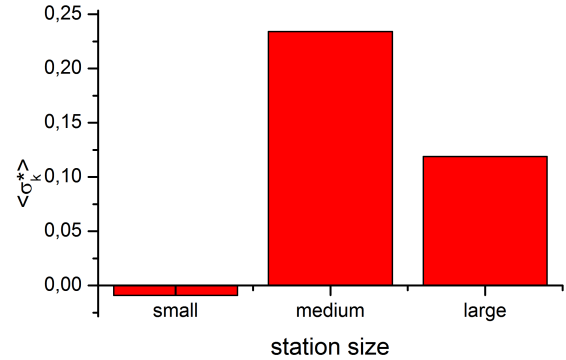


Fig. 14. Average σ^* for small, medium and large stations. The rank is split at 80 and 170 A/D events per day, respectively.

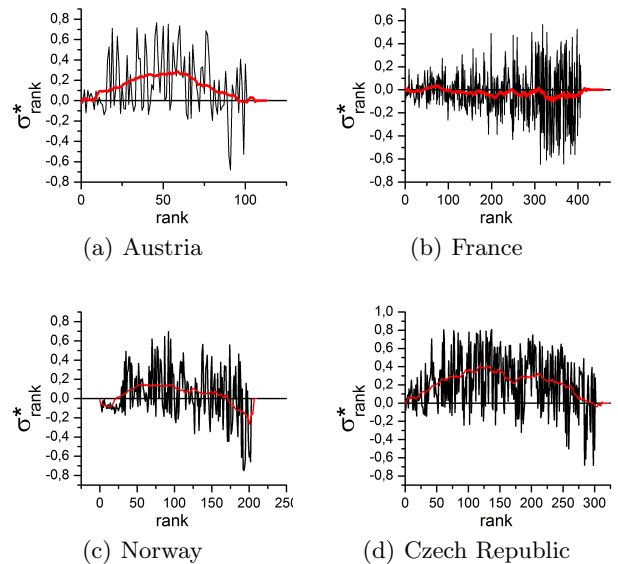


Fig. 15. The synchronization in the long-distance train connections of different European countries with $N_R = 100$ and an averaging window of 40.

ures 15(a)-15(d)). France shows only a very weak signal, whereas the shapes of the synchronization curves in Austria, Norway and the Czech Republic are very similar to the one observed in Germany (Figure 13).

In the following we will show results for the interdependencies of our main quantities b_k , $s_k(p)$ and σ_k^* . In all cases, like before, we compute local averages with respect to the rank. By grouping the stations according to their position in the b - $s(p)$ -plane, Figure 12, i.e. according to their robustness and efficiency, one can now study, whether stations from the same regions share a common synchronization index σ_k^* .

Figure 16 shows the average σ for the three regions containing stations. The stations from the most preferable region ++ show extremely low synchronization, while

those of the regions $+-$ and $--$ are much more synchronized.

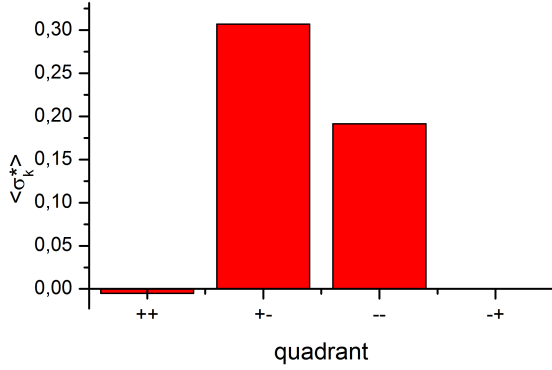


Fig. 16. Average synchronization of the stations grouped together by robustness and efficiency according to the quadrants in Figure 12.

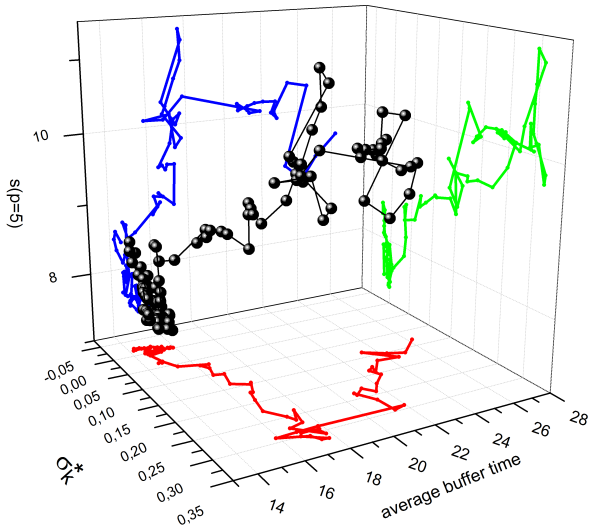


Fig. 17. Dependencies of buffering time b , secondary delay $s(p)$, and synchronization index σ_k^* .

In order to show the dependencies among these quantities more directly, Figure 17 represents all three quantities b_k , $s_k(p)$ and σ_k^* , simultaneously. The smoothing window size is set to 26. It is clearly visible that most stations are in the regions of low σ_k^* , low b_k and low $s_k(p)$. Furthermore, there is a clear correlation between $s_k(p)$ and σ_k^* and

consequently, an anti-correlation between synchronization and robustness.

4 Avalanche Model

Can the negative correlation between synchronization and robustness that we observe in the data also be understood in some minimal model of delay propagation? The general dynamical mechanism resembles some aspects of avalanches on graphs. While avalanche models are an important focus of interest in complex systems theory and in particular in the field of self-organized criticality [9, 2], we do not expect here a power-law distribution of event sizes, as the elementary processes behind delay propagation are different from the threshold-driven re-distribution schemes encoded, e.g. in the Bak-Tang-Wiesenfeld (BTW) model [3]. Therefore, we adapt the general concept of an avalanche model to the dynamical needs of delay propagation.

In our passenger delay avalanche model the dynamical variables are the accumulated delays $d_i(t)$ at node i as a function of time t . The model has three parameters:

(1) The transmission probability p is the probability that a delay propagates from one node to an adjacent node, if the threshold is crossed. This probability describes the capacity to buffer incoming delays via transfer times.

(2) The amplification factor m acknowledges the fact that a single train delay corresponds to multiple passenger delays; consequently, if a few incoming passengers cause a train with many outgoing passengers to wait, the total (passenger-based) delay is amplified. This parameter can be seen as the ratio of these passenger numbers, i.e. the average rate of additionally delayed passengers due to waiting.

(3) Delays only propagate from a node i to adjacent nodes, when the delay variable $d_i(t)$ is above a threshold T , as we assume that only incoming delays higher than this threshold are capable of triggering delay propagation. Figure 18 shows that the tail of the size distribution of delay avalanches is exponential.

In order to analyze the relation between synchronization and robustness within this model, we compare the average avalanche length for a system, where a single node is periodically driven, with the case of a stochastically driven node.

We assume that the gradual insertion of delay units into the system corresponds to incoming delays from other parts of the network entering the sub-network, which is here studied in detail. A periodic insertion of such delay units then corresponds to highly synchronized arrival/departure (A/D) events (as only those can give rise to periodic delays), while the stochastically driven node represents the typical pattern of incoming delays for a station with less synchronized A/D events.

Figure 19 shows the distribution of these average avalanche lengths for the two cases. The periodically driven node (high synchronization of A/D events) coincides with a high average size of the delay avalanches (i.e. higher vulnerability or lower robustness), while the stochastically

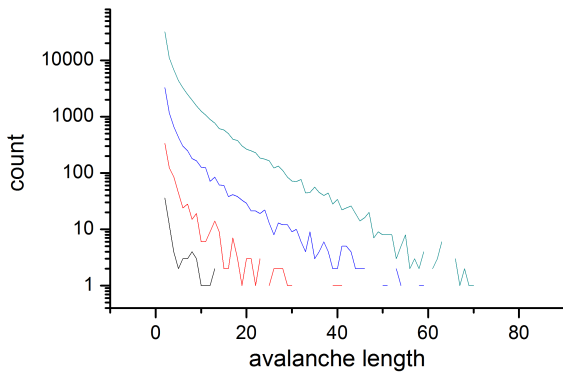


Fig. 18. The distribution of the avalanche lengths for stochastic and periodic drivers with a driving period of 17, $T = 4$, $m = 0.9$, $N = 70$ nodes and $M = 240$ edges.

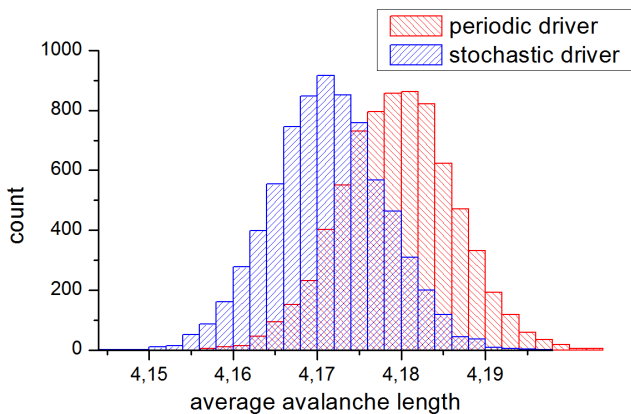


Fig. 19. The average avalanche length for stochastic and periodic drivers with a driving period of 17, $T = 4$, $m = 0.9$, $N = 70$ nodes and $M = 240$ edges.

driven node (low synchronization of A/D events) displays a lower average size of delay avalanches (and therefore a higher robustness). This is in agreement with the relationship discovered in the real train connection data studied in the previous section.

5 Conclusions

In this work we have studied railway timetables from a novel and yet unexplored view, namely that of phase synchronization. For our analysis we investigated the German long-distance train timetable with respect to three distinct properties: robustness, efficiency and phase synchronization.

The robustness reflects the stability of the system to small perturbations, while efficiency is related to short accumulated waiting times per train route. These two properties have been evolved over the years by gathered experience and heuristic optimization.

When we consider the arrival and departure events of all trains at a given station over a period of time, 24 hours

for example, we can translate those events into phases. Summing over all different phases we can compute a synchronization index for each station. Then, by exhaustive simulation we produce a primary delay at each station and record the induced secondary delays. Our results show a clear and surprising correlation between the synchronization index of a station, its robustness and efficiency.

In the Introduction, we have discussed the difference between car traffic in cities and the impact of traffic light synchronization on the one side and railway timetables on the other. It would be interesting to compare these two types of traffic in detail, to quantitatively analyze the number of directions (node degrees) in the context of an effective dimension, and in particular to study the complexity (given, e.g., by the pattern of elementary decisions needed to specify the path) of a typical path in the train network compared to the car traffic case. A suitable methodology could be the framework developed in [32].

The balance between this antagonistic pair of requirements, efficiency and robustness, is of broad interest across many disciplines, ranging from industrial production to biological processes. Lack of robustness due to too high efficiency is sometimes called the systemic risk, which has recently been discussed from a theoretical perspective, for example for complex economical systems (see [4, 5, 25]).

Starting from an information-theoretical description of resilience in ecology, Ulanowicz et al. [37] could establish quantitative links between sustainability, efficiency and investments in diversity. This general framework has been employed to analyze the current bank crisis from an ecosystem perspective [24]. We believe that a quantitative view on synchronization of arrival/departure events in the network of long-distance train connections, as presented here, can similarly serve as a starting point for a theoretical understanding, and subsequently systemic optimization, of the balance between efficiency and robustness for such timetables underlying public transportation.

For biological processes this balance between efficiency and robustness has been explored in a multitude of ways resorting to both analysis of experimental data and the mathematical modeling of cellular processes. Motivated by graph theory and nonlinear dynamics, an influential trend in systems biology at the moment is to relate robustness to small regulatory devices [1, 7], serving e.g. as a noise buffer or providing a suitable amount of redundancy for maintaining systemic function even under perturbations. In particular such relations between the architecture of regulatory devices and dynamical functions have been worked out for circuits of negative feedback loops [30], for feedforward loops as noise filtering devices in gene regulation [1, 35], for interlinked feedback loops acting on different time scales [6], for a particular composition of regulatory units [27] and their relation to robustness [13, 10, 11, 12], for number of positive and negative feedback loops in regulatory circuits [17].

It could well be that in the network of long-distance train connections such small, motif-like network components serve as mediators between synchronization, reliability and efficiency. Exploring the involvement of network

topology in shaping this relationship is one of our principal goals in the continuation of the work presented here.

References

1. U. Alon. Network motifs: theory and experimental approaches. *Nat Rev Genet*, 8:450–461, 2007.
2. P. Bak. *How Nature Works: The Science of Self-Organised Criticality*. Copernicus Press, New York, 1996.
3. P. Bak, C. Tang, and K. Wiesenfeld. Self-organized criticality: An explanation of the $1/f$ noise. *Phys. Rev. Lett.*, 59(4):381–384, Jul 1987.
4. S. Battiston, D. Delli Gatti, and M. Gallegati. Trade credit networks and systemic risk. In D. Helbing, editor, *Managing Complexity: Insights, Concepts, Applications*, pages 219–239. Springer, 2008.
5. S. Battiston, D. Delli Gatti, M. Gallegati, B. Greenwald, and J. Stiglitz. Credit chains and bankruptcy propagation in production networks. *Journal of Economic Dynamics and Control*, 31(6):2061–2084, 2007.
6. O. Brandman, J.E. Ferrell, R. Li, and T. Meyer. Interlinked fast and slow positive feedback loops drive reliable cell decisions. *Science*, 310:496, 2005.
7. O. Brandman and T. Meyer. Feedback loops shape cellular signals in space and time. *Science*, 322:390–395, 2008.
8. E. Brockfeld, R. Barlovic, A. Schadschneider, and M. Schreckenberg. Optimizing traffic lights in a cellular automaton model for city traffic. *Phys. Rev. E*, 64(5):056132, 2001.
9. H. J. Jensen. *Self-Organized Criticality: Emergent Complex Behavior in Physical and Biological Systems*. Cambridge University Press, 1998.
10. P. Kaluza, M. Ipsen, M. Vingron, and A. S. Mikhailov. Design and statistical properties of robust functional networks: A model study of biological signal transduction. *Phys. Rev. E*, 75:015101, 2007.
11. P. Kaluza and A. S. Mikhailov. Evolutionary design of functional networks robust against noise. *Europhys. Lett.*, 79:48001, 2007.
12. P. Kaluza, M. Vingron, and A. S. Mikhailov. Self-correcting networks: Function, robustness, and motif distributions in biological signal processing. *Chaos*, 18:026113, 2008.
13. K. Klemm and S. Bornholdt. Topology of biological networks and reliability of information processing. *PNAS*, 102:18414–18419, 2005.
14. L.G. Kroon, R. Dekker, and M.J.C.M. Vromans. Cyclic railway timetabling: a stochastic optimisation approach. In F. Geraets, L.G. Kroon, A. Schöbel, D. Wagner, and C. Zaroliagis, editors, *Algorithmic Methods in Railway Optimization*, volume 4359 of *Lecture Notes in Computer Science*, pages 41–66. Springer, 2007.
15. L.G. Kroon, D. Huisman, E.J.W. Abbink, P.J. Fioole, M. Fischetti, G. Maróti, A. Schrijver, A. Steenbeek, and R. Ybema. The new Dutch timetable: The OR revolution. *Interfaces*, 39(1):6–17, 2009.
16. Y. Kuramoto. *Chemical Oscillations, Waves, and Turbulence*. Springer, Berlin, 1984.
17. Y.-K. Kwon and K.-H. Cho. Quantitative analysis of robustness and fragility in biological networks based on feedback dynamics. *Bioinformatics*, 24:987–994, 2008.
18. S. Lämmer and D. Helbing. Self-control of traffic lights and vehicle flows in urban road networks. *Journal of Statistical Mechanics: Theory and Experiment*, 2008(04):P04019 (34pp), 2008.
19. S. Lämmer, H. Kori, K. Peters, and D. Helbing. Decentralised control of material or traffic flows in networks using phase-synchronisation. *Physica A: Statistical Mechanics and its Applications*, 363(1):39 – 47, 2006.
20. C. Liebchen. *Periodic timetable optimization in public transport*. PhD thesis, Technische Universität Berlin, 2006.
21. C. Liebchen. The first optimized railway timetable in practice. *Transportation Science*, 42:420–435, 2008.
22. C. Liebchen, M. Schachtebeck, A. Schöbel, S. Stiller, and A. Prigge. Computing delay resistant railway timetables. *Computers and Operations Research*, 37:857–868, 2010.
23. C. Liebchen and S. Stiller. Delay resistant timetabling. *Public Transport*, 1:55–72, 2009.
24. B. Lietaer, U. Ulanowicz, and S. Goerner. Options for managing a systemic bank crisis. *SAPIENS*, 2:1–15, 2009.
25. J. Lorenz, S. Battiston, and F. Schweitzer. Systemic risk in a unifying framework for cascading processes on networks. *European Physical Journal B*, 71:441–460, 2009.
26. S. C. Manrubia, A. S. Mikhailov, and D. H. Zanette. *Emergence of Dynamical Order, Synchronization Phenomena in Complex Systems*. World Scientific, 2004.
27. R. Milo, S. Itzkovitz, N. Kashtan, R. Levitt, S. Shen-Orr, I. Ayzenshtat, M. Sheffer, and U. Alon. Superfamilies of evolved and designed networks. *Science*, 303:1538, 2004.
28. M. Müller-Hannemann and M. Schnee. Efficient timetable information in the presence of delays. In R. K. Ahuja, R. H. Möhring, and C. D. Zaroliagis, editors, *Robust and Online Large-Scale Optimization: Models and Techniques for Transportation Systems*, volume 5868, pages 249–272. Springer, 2009.
29. L.W.P. Peeters. *Cyclic railway timetable optimization*. PhD thesis, Erasmus University Rotterdam, Rotterdam School of Management, The Netherlands, 2003.
30. S. Pigolotti, S. Krishna, and M.H. Jensen. Oscillation patterns in negative feedback loops. *PNAS*, 104:6533–6537, 2007.
31. A. Pikovsky, M. Rosenblum, and J. Kurths. *Synchronization: A Universal Concept in Nonlinear Sciences*. Cambridge University Press, 2003.
32. M. Rosvall, A. Grönlund, P. Minnhagen, and K. Sneppen. Searchability of networks. *Phys. Rev. E*, 72(4):046117, Oct 2005.
33. M. Schnee. *Fully Realistic Multi-Criteria Timetable Information*. PhD thesis, Technische Universität Darmstadt, Germany, 2009.
34. P. Serafini and W. Ukovich. A mathematical model for periodic event scheduling problems. *SIAM Journal on Discrete Mathematics*, 2:550–581, 1989.
35. S. Shen-Orr, R. Milo, S. Mangan, and U. Alon. Network motifs in the transcriptional regulation network of *escherichia coli*. *Nat Genet*, 31:64–68, 2002.
36. S. H. Strogatz. Exploring complex networks. *Nature*, 410(6825):268–276, 2001.
37. U. Ulanowicz, S. Goerner, B. Lietaer, and R. Gomez. Quantifying sustainability: Resilience, efficiency and the return of information theory. *Ecological Complexity*, 6:27–36, 2009.
38. J. Walleczek, editor. *Self-organized biological dynamics and nonlinear control*. Cambridge University Press, 2000.

39. A. T. Winfree. *The Geometry of Biological Time*. Springer, New York, 1980.